

Autoxidation of Ni(II) and Co(II) Tetra, Penta and Hexaglycine Complexes Accelerated by Oxy Sulfur Radicals

Luciana B. Carvalho, María V. Alipázaga, Denise Lowinsohn, Mauro Bertotti and Nina Coichev*

Instituto de Química, Universidade de São Paulo, CP 26077, 05513-970 São Paulo-SP, Brazil

A autoxidação dos complexos de Ni(II) e Co(II) com tetra, penta e hexaglicina, em meio de tampão borato, é acelerada por espécies de enxofre(IV) (H_2SO_3 , HSO_3^- and SO_3^{2-}). A formação dos complexos de Ni(III) e Co(III) foi acompanhada espectrofotometricamente em 325 e 265 nm, respectivamente. Técnicas eletroquímicas também foram empregadas para caracterizar a geração destes complexos. A velocidade da reação de autoxidação aumenta com a concentração de S(IV) e é máxima em $\text{pH} \cong 8,5$. O processo é autocatalítico com Ni(III) ou Co(III) atuando como iniciadores, formados pela oxidação espontânea de Ni(II) ou Co(II) pelo oxigênio molecular. A dependência da constante de velocidade de pseudo-primeira ordem com a concentração de sulfito evidenciou possíveis reações paralelas com formação de um complexo com ligantes mistos antes da etapa da oxidação.

The autoxidation of Ni(II) and Co(II) complexes with tetra, penta and hexaglycine, in borate medium, is accelerated by sulfur(IV) species (H_2SO_3 , HSO_3^- and SO_3^{2-}). The formation of Ni(III) and Co(III) complexes was followed spectrophotometrically at 325 and 265 nm, respectively. Electrochemical techniques were also employed to characterize the generation of these complexes. The autoxidation rate increases with S(IV) concentration and is maximum at $\text{pH} \cong 8.5$. The process is autocatalytic with Ni(III) or Co(III) acting as initiators, formed by spontaneous oxidation by oxygen. The dependence of the pseudo first order rate constant with sulfite concentration showed evidences of back or parallel reactions with formation of mixed ligand complex prior to the oxidation step.

Keywords: nickel, cobalt, pentaglycine, hexaglycine, sulfite

Introduction

The S(IV) induced autoxidation of Ni(II), Co(II) and Cu(II) in the presence of complexing medium, where the formation of the metal ion in the 3+ oxidation state can be followed, has been studied by our research group.¹⁻¹⁷ Detailed kinetics and mechanistic studies have been done for the systems: Co(II)/(III)/ N_3^- ,² Mn(II)/(III)/ N_3^- ,³ Fe(II)/(III)/ H_2O ,^{18,19} Mn(II)/(III)/ Ac^- ,⁹ Co(II)/(III)/TRIS,^{4,15} Ni(II)/(III)/cyclam,^{7,8} Ni(II)/(III)/ OH^- ,⁶ Ni(II)/(III)/tetraglycine,^{14,17} Co(II)/(III)/tetraglycine¹⁷ and Cu(II)/(III)/tetra, penta and hexaglycine.^{5,10,11,16}

The oxidation of S(IV) occurs simultaneously with the consumption of oxygen and oxidation of the metal ion complex to the 3+ oxidation state, which could be followed in a suitable complexing medium by spectrophotometric^{4,5,10,11,15-17} or amperometric¹³ methods.

Some sensitive analytical methods for S(IV) in air, rain water, juices, wines and white sugar have been developed based on the linear dependence of the concentration of the metal ion complex (at 3+ oxidation state) and the initial concentration of S(IV).^{4,5,10,11,14}

The S(IV) induced autoxidation of Ni(II) and Co(II) tetraglycine complexes is very fast.^{17,20} On the other hand, Cu(II) tetraglycine complexes react slowly but traces (10^{-6} mol L⁻¹) of Ni(II) and Co(II) ions accelerate the oxidation.¹⁶ The formation of Ni(III) and Co(III) tetraglycine complexes can be followed spectrophotometrically by absorbance changes at 325 and 265 nm, respectively.

This article reports additional information on the S(IV) induced autoxidation of Ni(II) and Co(II) tetra (G_4), penta (G_5) and hexaglycine (G_6) complexes. Some analytical potentialities and a comparative study on the reactivity of Ni(III) and Co(III) complexes are also described.

*e-mail: ncoichev@iq.usp.br

Experimental

Reagents

All reagents were of analytical grade (Merck or Sigma) and were used as received. Solutions were prepared by using deionised water purified with a Milli-Q Plus Water system (Millipore).

Stock solutions of sulfite (1.00×10^{-2} mol L⁻¹) were daily prepared by dissolving the Na₂S₂O₅ salt in water previously purged with nitrogen. Water was flushed with nitrogen for at least half an hour to remove dissolved oxygen. To prepare diluted solutions of sulfite, small volumes of the stock solutions were properly added to air saturated water. The sulfite content of the stock solution was determined by iodimetry.²¹

Ni(II) (0.200 mol L⁻¹) stock solution was prepared from the direct reaction of Ni (powder) (99.99%) with double distilled nitric acid.

Co(II) (0.965 mol L⁻¹) stock solution was prepared from the direct reaction of Co(II) carbonate with perchloric acid followed by standardization with EDTA.²²

Spectrophotometric measurements

The metal ion complex solutions containing [Ni(II)] = 4.0×10^{-4} mol L⁻¹ in borate medium 0.10 mol L⁻¹ (pH = 7.51 - 10.1) or [Co(II)] = 2.0×10^{-4} mol L⁻¹ in borate buffer 0.10 mol L⁻¹ (pH = 8.48 - 9.30); ionic strength 0.2 mol L⁻¹ (NaClO₄), were freshly prepared. Ni^{II}G_n and Co^{II}G_n solutions were prepared by dissolving tetraglycine (G₄), pentaglycine (G₅) or hexaglycine (G₆) in borate solution followed by the addition of Ni(II) or Co(II) solution (prepared to have 100% or 10% excess of peptide, respectively).

The kinetics was followed at the wavelength of maximum absorption of the Ni^{III}G_n or Co^{III}G_n complexes by using an HP8453A diode array spectrophotometer.

The data were obtained by mixing an equal volume of sulfite solution ($2.0 - 14$) $\times 10^{-5}$ mol L⁻¹ and the metal ion complex solution (in borate buffer) in a double compartment cell (0.875 cm optical path length quartz cell) for slow reactions. Pro-K.2000 Stopped-Flow Mixing Accessory was used for the experiments at short time intervals. The final concentrations after the mixture are indicated in all figures.

Air saturated solutions were employed in all experiments and the oxygen concentration was considered to be 2.5×10^{-4} mol L⁻¹.²³ Water was used as reference solution (blank).

A pHmeter Metrohm model 713 with a glass electrode (filled with sat. NaCl) was used in the pH measurements. The temperature was kept at 25.0 °C.

Electrochemical measurements

An Autolab PGSTAT 30 (Eco Chemie) bipotentiostat with the data acquisition software (GPES 4.8 version) was used. Experiments were done in an electrochemical cell with a Ag/AgCl (saturated KCl) and a platinum wire as reference and counter electrodes, respectively. Voltammetry with a rotating ring-disc electrode (RRDE) was carried out using an analytical rotator (AFMSRX) connected to the bipotentiostat. The glassy carbon/glassy carbon ring-disk electrodes (AFMT29) had the following dimensions: disk radius = 0.5613 cm, inner radius of the ring = 0.6248 cm and outer radius of the ring = 0.7925 cm. During rotating ring-disk electrode voltammetric experiments, the disk electrode potential was scanned between the limits 0.2 and 1.0 V, the ring being maintained at 0.0 V to collect the material generated at the disk. 0.05 mol L⁻¹ NaClO₄ in borate buffer was used as supporting electrolyte.

The voltammograms were obtained from air saturated solutions containing the metal ion complexes in borate buffer. In order to evaluate the effect of S(IV) on the voltammetric profile, very small volumes of S(IV) solutions were added to the electrochemical cell. The S(IV) concentration in the final solutions is indicated in the figures.

Results and Discussion

The sulfite induced autoxidation of Ni^{II}G_n

Ni^{II}G_n complexes have maximum absorbance peaks at 250 and 410 nm. In the case of Ni^{II}G₄ complex, literature²⁴ reports an equilibrium between the blue octahedral [Ni^{II}G₄]⁺ and the yellow square planar [Ni^{II}(H₃G₄)]²⁻ complexes. The amount of [Ni^{II}(H₁G₄)] and [Ni^{II}(H₂G₄)]⁻ in solution is not appreciable at pH = 9.0 (H₋₁G_n²⁻, H₋₂G_n³⁻ and H₋₃G_n⁴⁻ refer to the peptide ligand with 1, 2 and 3 deprotonated peptide nitrogen coordinated to nickel ion). In the present work, the transition from the octahedral to the square-planar geometry could be followed at 250 nm by the absorbance increasing, a constant value being reached after 10 minutes.

Ni^{II}G₅ (2.0×10^{-4} mol L⁻¹) reacts slowly with oxygen in an autocatalytic process with induction period of 10000 s (at pH=8.50, borate buffer). However, in the presence of S(IV) the formation of Ni^{III}G₅ complexes becomes much faster and reaches an absorbance limit after 1 s.

The S(IV) induced autoxidation of Ni^{II}G_n complexes was studied following the absorbance changes at 325 nm.

Figure 1A and 1A' show the spectra obtained before and after 0.8 s of addition of $5.0 \times 10^{-5} \text{ mol L}^{-1}$ sulfite to a $\text{Ni}^{\text{II}}\text{G}_5$ solution. An absorption band at 325 nm is observed due to the formation of $\text{Ni}^{\text{III}}\text{G}_5$.

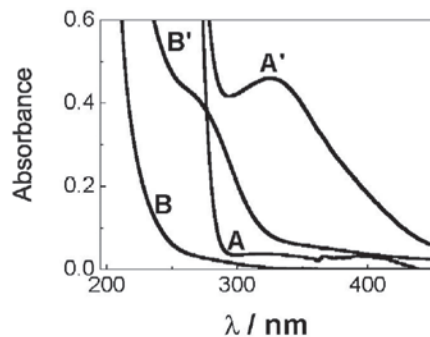


Figure 1. Spectral changes before (A, B) and after (A', B') addition of $5.0 \times 10^{-5} \text{ mol L}^{-1}$ sulfite to the solution of metal ion complex. $[\text{Ni}^{\text{II}}\text{G}_5]$ (A, A' - after 0.8 s) = $2.0 \times 10^{-4} \text{ mol L}^{-1}$; $[\text{G}_5] = 2.0 \times 10^{-4} \text{ mol L}^{-1}$; [borate buffer] = 0.050 mol L^{-1} (pH = 8.50); T = 25.0°C . Or $[\text{Co}^{\text{II}}\text{G}_5]$ (B, B' - after 1800 s) = $1.0 \times 10^{-4} \text{ mol L}^{-1}$; $[\text{G}_5] = 0.10 \times 10^{-4} \text{ mol L}^{-1}$; [borate buffer] = 0.050 mol L^{-1} (pH = 9.05); T = 25.0°C .

Figure 2 shows the effect of the medium acidity on the formation and decomposition of $\text{Ni}^{\text{III}}\text{G}_5$. The maximum absorbance is reached at approximately 0.8 s as result of the fast S(IV) induced autoxidation of $\text{Ni}^{\text{II}}\text{G}_5$ complex; a maximum value was observed at pH=8.50. The further decomposition of $\text{Ni}^{\text{III}}\text{G}_5$ complex increases with the increase of the pH, a similar behavior being observed with $\text{Ni}^{\text{II}}\text{G}_4$ and $\text{Ni}^{\text{II}}\text{G}_6$ complexes. The $\text{Ni}^{\text{II}}\text{G}_4$ complex formed in absence of sulfite decomposes with oxidation of the ligand.²⁰

The Olis Kinfite²⁵ and Pro-K.2000²⁶ set of programs were employed to fit the absorbance-time traces. However, no good approach was achieved. Therefore, the first order formation of $\text{Ni}^{\text{III}}\text{G}_n$ (k_{obs}) was obtained by the initial slope ($\ln(\text{Absorbance}_t) - \ln(\text{Absorbance}_i)$) vs. time plots, neglecting the induction period (less than 0.1 s). Unfortunately, the software from Pro-K.2000 Stopped-Flow Mixing Accessory (on line with HP8453A diode array spectrophotometer) allows data acquisition with time interval of 0.1 s, such as after the induction period only three or four points were available to obtain the initial slope. This part of the kinetic trace exhibits the maximum rate for $\text{Ni}^{\text{III}}\text{G}_n$ formation.^{2,27}

The k_{obs} vs. pH, represented in Figure 2(B), can be subject of some error due to the interference of the induction period (an evidence of autocatalytic process) and further decomposition of $\text{Ni}^{\text{III}}\text{G}_5$ complex (especially at higher pH). k_{obs} values increase with pH in the range of 7.5 – 9.0 likely because of the different degree of protonation of the nickel complexes, which is

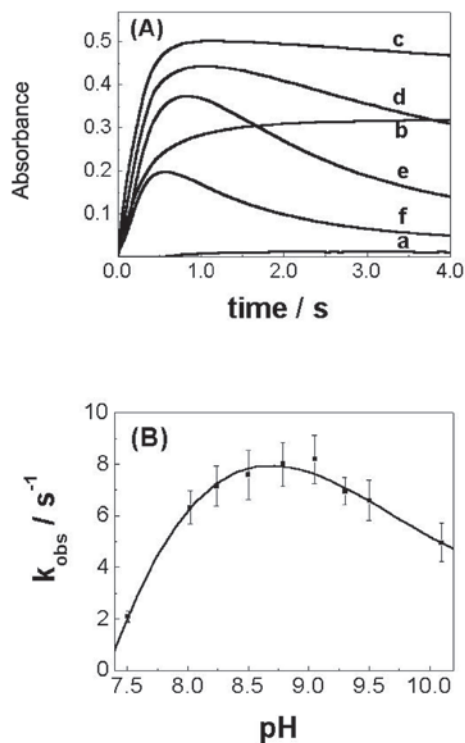


Figure 2. (A) Effect of pH. Absorbance changes at 325 nm for the sulfite induced autoxidation of $\text{Ni}^{\text{II}}\text{G}_5$ complex. (B) k_{obs} as a function of pH for the sulfite induced autoxidation of $\text{Ni}^{\text{II}}\text{G}_5$ complex. $[\text{Ni}^{\text{II}}\text{G}_5] = 2.0 \times 10^{-4} \text{ mol L}^{-1}$; $[\text{G}_5] = 2.0 \times 10^{-4} \text{ mol L}^{-1}$; [borate buffer] = 0.050 mol L^{-1} ; $[\text{S(IV)}] = 5.0 \times 10^{-5} \text{ mol L}^{-1}$; $I = 0.1 \text{ mol L}^{-1}$; T = 25.0°C . pH = (a) 7.51; (b) 8.02; (c) 8.50; (d) 9.05; (e) 9.50; (f) 10.1.

dependent on the medium acidity. The $[\text{Ni}^{\text{II}}(\text{H}_3\text{G}_5)]^{2-}$ is probably the main species in solution at pH 8.5 – 9.0.

For instance, the pK_3 for $\text{Ni}^{\text{II}}\text{G}_4$ ($[\text{Ni}^{\text{II}}(\text{H}_3\text{G}_4)]^{2-}$). $[\text{H}^+]/[\text{Ni}^{\text{II}}(\text{H}_2\text{G}_4)]^-$ is 8.1²⁰ showing that at this pH the ratio $[\text{Ni}^{\text{II}}(\text{H}_2\text{G}_4)]^- : [\text{Ni}^{\text{II}}(\text{H}_3\text{G}_4)]^{2-}$ is 1:1. At pH = 8.5, the predominant specie of Ni(III) complexes must be $[\text{Ni}^{\text{III}}(\text{H}_3\text{G}_4)]^-$.

For comparative studies, a kinetic investigation on the S(IV) induced autoxidation of $\text{Ni}^{\text{II}}\text{G}_n$ complexes was carried out at pH=8.50, in air saturated solution. At this pH, the Ni(III) formation was more efficient and its decomposition is slower (Figure 2(A)).

The dependence of $\text{Ni}^{\text{III}}\text{G}_5$ formation on the S(IV) concentration (Figure 3(A)) could only be studied over a limited concentration range where the initial $[\text{S(IV)}] = (0.05 - 0.35) \times [\text{Ni(II)}]$. At $[\text{S(IV)}] > 7 \times 10^{-5} \text{ mol L}^{-1}$ the reduction of $\text{Ni}^{\text{III}}\text{G}_5$ formed may occur in an air saturated solution ($[\text{O}_2] \cong 2.5 \times 10^{-4} \text{ mol L}^{-1}$).²³ Experiments following $\text{Ni}^{\text{III}}\text{G}_4$ and $\text{Ni}^{\text{III}}\text{G}_6$ formation showed similar Absorbance \times time profiles (data not shown). Experiments at $[\text{S(IV)}]$ lower than $1 \times 10^{-5} \text{ mol L}^{-1}$ would better define the intercept observed in the Figure 3(B), which is due to either a back or parallel reaction. However, the absorbance changes at

such lower S(IV) concentrations were not significant. Due to the lack of sufficiently detailed experimental information, the proposed kinetic data treatment yields a semi-quantitative description. Therefore, in the present work only the main pathways in the intrinsic mechanism are described.

Figure 3(A) shows a small induction period, which depends on the initial [S(IV)]. Absorbance values after 1 s are linear with initial [S(IV)], hence they may be used for analytical purposes. At longer scale ($t > 3$ s) the absorbance decreases as a consequence of the decomposition of $\text{Ni}^{\text{III}}\text{G}_n$ complexes.

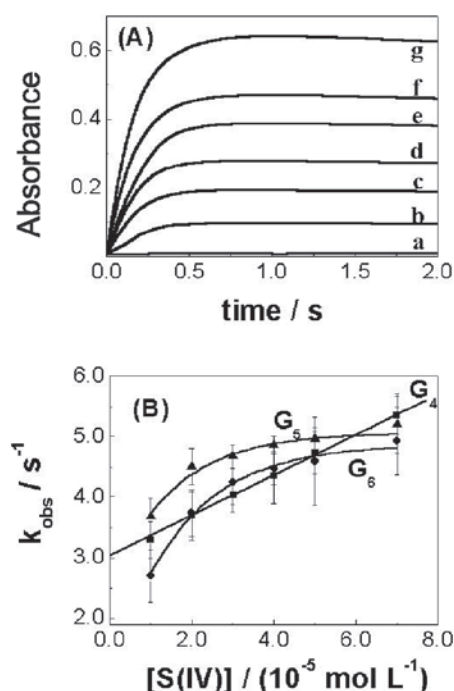


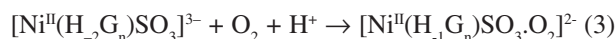
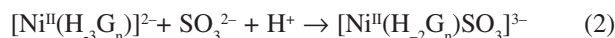
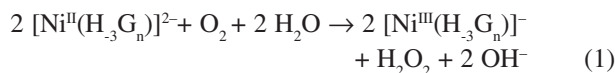
Figure 3. Effect of [S(IV)]. (A) Absorbances changes at 325 nm for the sulfite induced autoxidation of $\text{Ni}^{\text{II}}\text{G}_5$ complex. (B) k_{obs} for the sulfite induced autoxidation of $\text{Ni}^{\text{II}}\text{G}_n$ complex. $[\text{Ni}^{\text{II}}\text{G}_n] = 2.0 \times 10^{-4} \text{ mol L}^{-1}$; $[\text{G}_n] = 2.0 \times 10^{-4} \text{ mol L}^{-1}$; [borate buffer] = 0.050 mol L^{-1} ; pH = 8.50; $I = 0.1 \text{ mol L}^{-1}$; $T = 25.0^\circ\text{C}$. [S(IV)] = (a) zero; (b) 1.0×10^{-5} ; (c) 2.0×10^{-5} ; (d) 3.0×10^{-5} ; (e) 4.0×10^{-5} ; (f) 5.0×10^{-5} ; (g) $7.0 \times 10^{-5} \text{ mol L}^{-1}$.

Mechanism

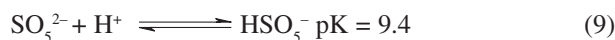
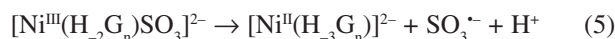
As already shown in our previous work,^{7,17} the sulfite induced autoxidation of $\text{Ni}^{\text{II}}\text{G}_4$ is an autocatalytic process involving a chain of redox reactions with free radical formation.

The Scheme 1 describes the main reactions involving a redox cycling for the oxidation of $\text{Ni}^{\text{II}}\text{G}_n$ complexes promoted by the strong oxidizing agents ($\text{SO}_4^{\cdot-}$, $\text{SO}_5^{\cdot-}$ and HSO_5^-) generated in the reaction.

Initiation



Autocatalysis



Scheme 1. Mechanism of the sulfite induced autoxidation of $\text{Ni}^{\text{II}}\text{G}_n$,¹⁷ where $\text{H}_{-1}\text{G}_n^{2-}$, $\text{H}_{-2}\text{G}_n^{3-}$ and $\text{H}_{-3}\text{G}_n^{4-}$ refer to the peptide ligand with 1, 2 and 3 deprotonated peptide nitrogen coordinated to the nickel ion.

The autocatalytic process needs the initiator $\text{Ni}^{\text{III}}\text{G}_n$ to start the reaction (equation 6). Small amounts of this species are produced by direct oxidation of $\text{Ni}^{\text{II}}\text{G}_n$ by dissolved oxygen (equation 1).^{17,20} This step initiates the reaction between $\text{Ni}^{\text{III}}\text{G}_n$ and SO_3^{2-} (equation 6) with formation of $\text{SO}_3^{\cdot-}$, which reacts with O_2 producing $\text{SO}_5^{\cdot-}$ (equation 7). The oxidation of $\text{Ni}^{\text{II}}\text{G}_n$ occurs with simultaneous consumption of O_2 ^{6,8,9} and S(IV) oxidation. The balance of S(IV) and O_2 controls the redox cycling process.^{2,3,6,8,18,19,28-36} In this process type the interaction of the metal ion (such as Fe^{3+} , Mn^{3+} , Co^{3+} and Ni^{3+}) with HSO_3^- or SO_3^{2-} , at low concentrations, results in the oxidation of SO_3^{2-} to the radical $\text{SO}_3^{\cdot-}$ and the reduction of the metal ion to the 2+ state. In the presence of oxygen, the metal ion is oxidized back to higher oxidation state. This redox cycling was clearly demonstrated for $\text{Co(II)/(III)/N}_3^-$,³³ $\text{Mn(II)/(III)/N}_3^-$,³³ $\text{Fe(II)/(III)/H}_2\text{O}$,³² Ni(II)/(III)/OH^- ,⁶ $\text{Ni(II)/(III)/cyclam}$.⁸

Some studies in the literature^{9,31} clearly show the importance of Fe(III) as one possible initiator, present as unavoidable impurity in chemicals or even in highly purified water. If Fe(III) is considered as the initiator, $\text{SO}_3^{\cdot-}$ could be generated by the reduction of Fe(III) by SO_3^{2-} (similar to equation 6), with further oxidation of $\text{Ni}^{\text{II}}\text{G}_n$ (equations 8, 10-12). As the present studies were carried out at pH = 8.50, Fe(III) impurities may be present as hydrolyzed species and equation 6 must be important in the initiation process.

The intercept and constant value of k_{obs} at higher S(IV) concentration (in the case of $\text{Ni}^{\text{II}}\text{G}_5$ and $\text{Ni}^{\text{II}}\text{G}_6$ autoxidation) in Figure 3(B) can be interpreted as an evidence of back or parallel reaction, as represented by equation 5. The formation of mixed ligand complex (equations 2 and 3), prior to the oxidation step (equation 4), may involve a slow dechelation process of the G_n ligand with coordination of sulfite and O_2 to $\text{Ni}^{\text{II}}\text{G}_n$. An internal electron transfer could produce $[\text{Ni}^{\text{III}}(\text{H}_2\text{G}_n)\text{SO}_3]^{2-}$ (equation 4). In a posterior step Ni(III) is reduced by SO_3^{2-} to give $[\text{Ni}^{\text{II}}(\text{H}_3\text{G}_n)]^{2-}$ and $\text{SO}_3^{\cdot-}$.

Two studies in the literature about Ni(II)/(III) peptide complex are relevant in the present discussion. Lepentisotis *et al.*³⁶ proposed the formation of $\text{Ni}^{\text{III}}\text{L}(\text{SO}_4^{\cdot-})$ (L=lysylglycylhistidine carboxiamide), where the $\text{SO}_4^{\cdot-}$ radical may coordinate to $\text{Ni}^{\text{III}}\text{L}$ complex. Green *et al.*³⁷ considered the formation of reactive dimmer species of Ni(II) and Ni(III) $\text{Gly}_2\text{HisGly}$ complexes in the oxidative self-decomposition of Ni(III) complex.

The sulfite induced autoxidation of $\text{Co}^{\text{II}}\text{G}_n$

Figure 1B shows the spectrum of a $\text{Co}^{\text{II}}\text{G}_5$ solution (pH = 9.05) recently prepared. The $\text{Co}^{\text{III}}\text{G}_5$ formation in air saturated solution, in absence or presence of S(IV), can be followed by the absorbance changes at 265 nm (Figure 1B').

A solution of $1.0 \times 10^{-4} \text{ mol L}^{-1}$ of $\text{Co}^{\text{II}}\text{G}_n$ complexes was chosen for the kinetic studies since $\text{Co}(\text{OH})_3$ may be formed at higher concentrations of Co(II) after 120 minutes. The precipitation of $\text{Co}(\text{OH})_3$ could also be prevented by keeping G_n ligand in excess (10%).

In the absence of sulfite the autoxidation of $\text{Co}^{\text{II}}\text{G}_5$ is relatively slow and becomes faster by increasing the pH (Figure 4(A)). At pH 8.48 – 9.05 (Figure 4(B) a-c) the effect of S(IV) by accelerating $\text{Co}^{\text{III}}\text{G}_5$ formation can be better evaluated (compare Figure 4(A) and 4(B)), since the spontaneous oxidation by dissolved oxygen is slower.

Similarly to $\text{Ni}^{\text{II}}\text{G}_n$ complexes, the reaction rate and effectiveness of Co(III) formation may be related to the

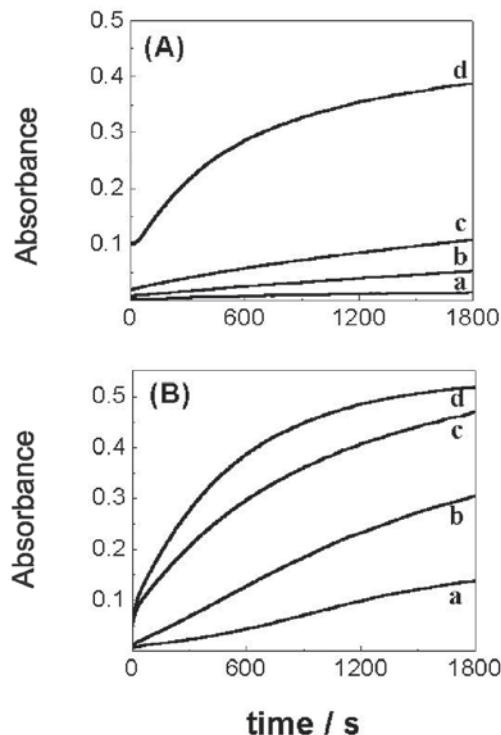


Figure 4. Effect of pH. Absorbances changes at 265 nm for the autoxidation of $\text{Co}^{\text{II}}\text{G}_5$ complex in the absence of S(IV) (A) and in the presence of S(IV) (B). $[\text{Co}^{\text{II}}\text{G}_5] = 1.0 \times 10^{-4} \text{ mol L}^{-1}$; $[\text{G}_5] = 0.10 \times 10^{-4} \text{ mol L}^{-1}$; $[\text{S(IV)}] = 5.0 \times 10^{-5} \text{ mol L}^{-1}$; [borate buffer] = 0.050 mol L^{-1} ; $I = 0.1 \text{ mol L}^{-1}$; $T = 25.0 \text{ }^\circ\text{C}$. pH = (a) 8.48; (b) 8.79; (c) 9.05; (d) 9.30.

different reactive species of $\text{Co}^{\text{II}}\text{G}_5$ due to the different protonation degree of the coordinated ligand, which is dependent on the solution acidity. As pK values for $[\text{Co}^{\text{II}}(\text{H}_x\text{G}_n)]^{(1-x)}$ or $[\text{Co}^{\text{III}}(\text{H}_x\text{G}_n)]^{(2-x)}$ are unknown, it is not possible to define the distribution diagram of the different species in the solution. Besides, a shift in the $\text{HSO}_3^-/\text{SO}_3^{2-}$ equilibrium ($\text{pK}_2 = 7.2$)³⁸ will lead to an increase in the redox rate constant at $\text{pH} > 7$.

The spontaneous oxidation of $\text{Co}^{\text{II}}\text{G}_n$ by dissolved oxygen was faster by increasing the pH, $\text{Co}^{\text{II}}\text{G}_n$ and ligand concentrations. For instance, the $\text{Co}^{\text{III}}\text{G}_n$ formation in the presence or absence of sulfite exhibits a remarkable dependence on the free ligand concentration (G_5 was kept in excess 0 – 200% over $\text{Co}^{\text{II}}\text{G}_5$, data not shown), the reaction becoming faster with higher $\text{Co}^{\text{III}}\text{G}_5$ formation.

In order to better evaluate the accelerating effect of S(IV) on the $\text{Co}^{\text{III}}\text{G}_n$ formation, experimental conditions must be such that the spontaneous oxidation by O_2 is minimized (Figure 5, $[\text{S(IV)}] = \text{zero}$) and the S(IV) effect is more pronounced.

Comparing $\text{Ni}^{\text{II}}\text{G}_5$ and $\text{Co}^{\text{II}}\text{G}_5$ ($[\text{M}^{\text{II}}\text{G}_5] = 1.0 \times 10^{-4} \text{ mol L}^{-1}$, 100% G_5 in excess, at pH = 9.05, data not shown), the later reacts faster with O_2 (in absence of S(IV)). However, Co(III) complexes formation is much slower in the presence of sulfite (compare Figures 3(A)

and 5(B)). $\text{Co}^{\text{III}}\text{G}_n$ complexes seem to be stable for 20 hours (the monitored time) since the absorbance at 265 nm does not change.

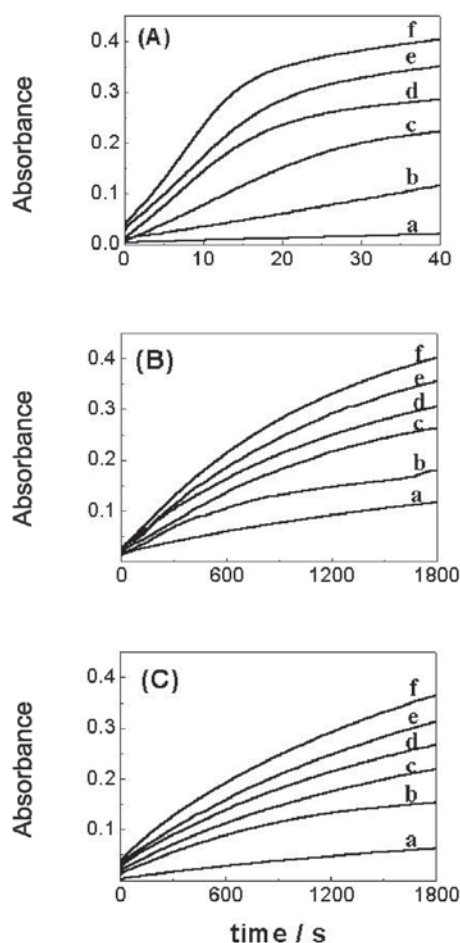


Figure 5. Effect of $[\text{S(IV)}]$. Absorbances changes at 265 nm for the sulfite induced autoxidation of $\text{Co}^{\text{II}}\text{G}_n$ complex, $\text{G}_n =$ (A) G_4 ; (B) G_5 ; (C) G_6 ; $[\text{Co}^{\text{II}}\text{G}_n] = 1.0 \times 10^{-4} \text{ mol L}^{-1}$; $[\text{G}_n] = 0.10 \times 10^{-4} \text{ mol L}^{-1}$; [borate buffer] = 0.050 mol L^{-1} ; pH = 9.05; $I = 0.1 \text{ mol L}^{-1}$; $T = 25.0^\circ\text{C}$. $[\text{S(IV)}] =$ (a) zero; (b) 1.0×10^{-5} ; (c) 2.0×10^{-5} ; (d) 3.0×10^{-5} ; (e) 4.0×10^{-5} ; (f) $5.0 \times 10^{-5} \text{ mol L}^{-1}$.

Figure 5 shows no clear induction period, which may indicate the formation of a significant amount of Co(III) as a result of spontaneous oxidation by oxygen.

Also in this case, the dependence of Co(III) formation with S(IV) concentration was studied over a limited concentration range $[\text{S(IV)}] = (0.1-0.5) \times [\text{Co(II)}]$. The experiments were not carried out under pseudo-first order conditions (Co(II) and O_2 in large excess over S(IV)).

The Olis Kinfit²⁵ set of program was employed to fit the absorbance-time traces and two exponential functions could be fitted (Table 1), resulting $k_{1\text{obs}}$ and $k_{2\text{obs}}$. It means that there are at least two consecutive steps, with rate constant values with different order of magnitude. However, it was not possible to fit the

Table 1. $k_{1\text{obs}}$ and $k_{2\text{obs}}$ for the sulfite induced autoxidation of $\text{Co}^{\text{II}}\text{G}_n$. $[\text{Co}^{\text{II}}\text{G}_n] = 1.0 \times 10^{-4} \text{ mol L}^{-1}$; $[\text{G}_n] = 0.10 \times 10^{-4} \text{ mol L}^{-1}$; [borate buffer] = 0.050 mol L^{-1} ; pH = 9.05; $I = 0.1 \text{ mol L}^{-1}$; $T = 25.0^\circ\text{C}$

$[\text{S(IV)}] /$ ($10^{-5} \text{ mol L}^{-1}$)	$\text{Co}^{\text{II}}\text{G}_4$ $k_{1\text{obs}} / 10^{-2} \text{ s}^{-1}$	$\text{Co}^{\text{II}}\text{G}_5$ $k_{1\text{obs}} / 10^{-3} \text{ s}^{-1}$	$\text{Co}^{\text{II}}\text{G}_6$ $k_{1\text{obs}} / 10^{-4} \text{ s}^{-1}$
1.0	1.3 ± 0.6	1.0 ± 0.3	5.8 ± 0.7
2.0	3.2 ± 0.9	0.85 ± 0.06	6.1 ± 0.8
3.0	5.4 ± 0.9	0.9 ± 0.2	5.2 ± 0.5
4.0	6.2 ± 1.5	0.80 ± 0.06	5.5 ± 0.6
5.0	8.6 ± 1.3	0.77 ± 0.03	5.9 ± 0.6
$k_{2\text{obs}} / \text{s}^{-1}$	2.0×10^{-3}	3.8×10^{-5}	3.6×10^{-5}

complete absorbance vs time trace with three or four exponential functions.

For $\text{Co}^{\text{II}}\text{G}_4$ complex, $k_{1\text{obs}}$ showed a dependence with S(IV) , while $k_{2\text{obs}} = 2.0 \times 10^{-3} \text{ s}^{-1}$ was found to be constant. These results are in agreement with our previous work.¹⁷ $k_{1\text{obs}}$ and $k_{2\text{obs}}$ do not depend on S(IV) concentration for $\text{Co}^{\text{II}}\text{G}_5$ and $\text{Co}^{\text{III}}\text{G}_6$ complexes formation.

The fact that the sulfite induced autoxidation of $\text{Co}^{\text{II}}\text{G}_4$ is faster than $\text{Co}^{\text{II}}\text{G}_5$ and $\text{Co}^{\text{II}}\text{G}_6$ complex could be associated to a steric effect of the ligands.

The $\text{Co}^{\text{III}}\text{G}_n$ formation, especially in the case of $\text{Co}^{\text{III}}\text{G}_5$ (Figure 5(B)) and $\text{Co}^{\text{III}}\text{G}_6$ (Figure 5(C)), is the sum of spontaneous oxidation by dissolved oxygen and S(IV) accelerating effect. Initially, the sulfite induced autoxidation of $\text{Co}^{\text{II}}\text{G}_n$ occurs with simultaneous oxidation of S(IV) . After the S(IV) consumption, the autocatalytic $\text{Co}^{\text{III}}\text{G}_n$ formation is due to the oxygen still remaining in solution (the absorbance did not reach a limit value).

The sulfite induced autoxidation of $\text{Co}^{\text{II}}\text{G}_n$ complexes also shows evidence for a mechanism involving formation of radicals. The initiation may also involve a parallel reaction with formation of a mixed ligand complex. Accordingly, literature shows that $\text{Co}^{\text{II}}\text{SO}_3^{2-}$ is fairly stable.³⁹

In the Scheme 1 (proposed for the sulfite induced autoxidation of $\text{Ni}^{\text{II}}\text{G}_n$), additional steps must be considered in the initiation process for $\text{Co}^{\text{III}}\text{G}_n$ generation, with formation of dimeric complexes with oxygen adduct and peroxo bridges.

Studies⁴⁰ with Co(II) peptides (gly-gly, gly-ala, ala-gly and ala-ala) showed the formation of dimeric complexes with μ -superoxo bridges. In the case of Co^{II} asparagine, the formation of dioxygen complex occurs prior to the oxidation of the metal center.⁴¹

The pH dependence of $\text{Co}^{\text{II}}\text{G}_n$ oxidation by oxygen (in the presence or absence of sulfite), Figure 4, may be explained by the possible formation of oxygen adduct or μ -superoxo bridge. This property of $\text{Co(II)}/(\text{III})$ complexes may explain the different behavior of $\text{Co}^{\text{II}}\text{G}_n$ compared to $\text{Ni}^{\text{II}}\text{G}_n$ in the presence of oxygen and sulfite.

Electrochemical studies of the oxidation of Ni^{II}G₄ and Co^{II}G₄

The voltammetric behavior of Ni^{II}G₄ complexes (in borate medium pH=9) has been already described in a previous work.¹⁷ Data obtained in this work suggested that the electrochemical process is reversible, the electrogenerated Ni^{III}G₄ is not stable in solution (see Figure 2d) and it is decomposed via ligand oxidation. Rotating ring-disk electrode voltammetry was used to characterize the degradation reaction of the Ni^{III}G₄ generated species.

We have extended in this work the investigation of the electroodic process of Ni(II) penta and hexaglycine complexes. Figure 6(a) shows RRDE voltammograms of a Ni^{II}G₅ solution; from the analysis of the data it is possible to conclude that a free-soluble species is generated during the sweep to positive potentials owing to the signal appearance at the ring. The anodic wave and the concurrent cathodic wave are one-electron processes represented by equations 13 and 15.

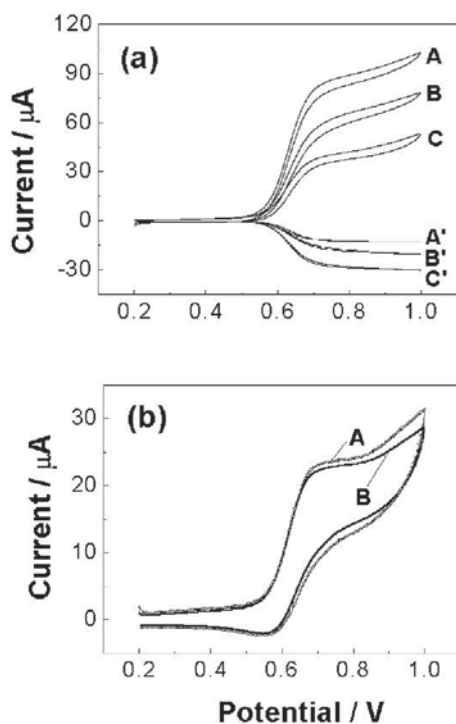
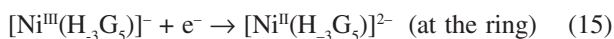


Figure 6. Current responses in RRDE experiments. [Ni^{II}G₅] = 2.0 × 10⁻⁴ mol L⁻¹, [G₅] = 0.2 × 10⁻⁴ mol L⁻¹; [borate buffer] = 0.050 mol L⁻¹ (pH = 8.5); NaClO₄ = 0.1 mol L⁻¹. (a) A, B, C: voltammograms recorded at the disk; A', B', C': at the ring (E = 0.0 V) at ω = 400, 1600 and 3600 rpm respectively. Scan rate = 20 mV s⁻¹. (b) Voltammograms recorded at the disk after addition of sulfite solution (A) zero and (B) 1.0 × 10⁻⁴ mol L⁻¹.

Similar results were obtained by carrying out the electrochemical experiments in solutions containing hexaglycine (results not shown). Data from this work are similar to those reported in the Ni^{II}G₄ system by analyzing both the existence of an anodic signal at around 0.6 V vs. Ag/AgCl and the formation of a Ni(III) complex in solution.

The collection efficiency (N), defined as the ratio of the limiting current values measured at the ring and the disk electrodes, indicates the amount of material electrogenerated at the disk that reaches the ring. Typical N values for Fe(CN)₆³⁻ (an electroactive species whose cathodic reduction leads to the stable Fe(CN)₆⁴⁻ anion) are close to 0.37; it is necessary to point out that in the Fe(CN)₆³⁻/Fe(CN)₆⁴⁻ system any subsequent chemical reaction occurs after the generation of Fe(CN)₆⁴⁻. Collection efficiency (N) values were measured for the Ni^{II}G₄, Ni^{II}G₅ and Ni^{II}G₆ systems and the respective values ranged from 0.22 to 0.27, 0.29 to 0.32 and 0.25 to 0.31, by performing experiments at different rotation rate values (400 to 3600 rpm); these results indicate that degradation of the electrogenerated Ni(III) complexes occurs during the transport to the ring (equation 14), as previously suggested for the Ni^{II}G₄ system.

Upon addition of S(IV) to solutions containing Ni^{II}G₆ no significant change was observed in the voltammetric profile, a comparable behavior being observed when experiments were performed in medium containing Ni^{II}G₅. These results suggest that the small amount of Ni^{III}G₆, probably is converted to the same Ni(II) complex during the timescale of the experiment, justifying the superposition of voltammetric curves in Figure 6(b). It should be pointed out that in the Ni^{II}G₄ system a small decrease in the anodic signal was observed,¹⁷ that would suggest a different pathway for the Ni(III) degradation in solutions containing G₄.

Voltammetric experiments were also carried out for solutions containing Co^{II}G₅ and Co^{II}G₆. Similar results as those described in the Co^{II}G₄ system were observed, *i.e.*, an irreversible anodic process with peak potential around 0.5 V.¹⁷ After addition of S(IV) a decrease in the anodic response was observed for both Co^{II}G₅ and Co^{II}G₆ complexes, as shown in the voltammetric cycles in Figure 7. This is an evidence of the chemical formation of some Co(III) complex, which is electro inactive at the potential range studied. As previously discussed, there is also a possible formation of a mixed ligand complex between Co^{II}G₅ and SO₃²⁻ in the solution, prior to the Co^{II} oxidation. The slight shift of the half wave potential by increasing S(IV) concentration can be an evidence of the different

nature of the Co(II) electroactive species still remaining in the solution.

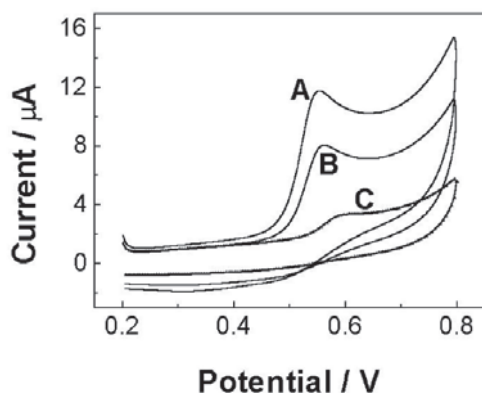


Figure 7. Voltammograms recorded at the disk after addition of S(IV) solution [S(IV)] = (A) zero, (B) 1.0×10^{-4} mol L $^{-1}$ and (C) 3.0×10^{-4} mol L $^{-1}$. [Co II G $_n$] = 1.0×10^{-4} mol L $^{-1}$, [G $_n$] = 0.1×10^{-4} mol L $^{-1}$; [borate buffer] = 0.05 mol L $^{-1}$ (pH = 9.0); NaClO $_4$ = 0.1 mol L $^{-1}$. Scan rate = 20 mV s $^{-1}$.

Conclusions

In the present work the formation of Ni(III) and Co(III) complexes could be followed by spectrophotometry and cyclic voltammetry. The exact nature of these complexes and of the products (structures, protonation degree of the ligands and mixed complexes) is unknown.

The complexity of the system does not allow a definitive assignment of the involved species. The redox process is more effective when oxygen is kept in large excess over sulfite concentration and higher pH. An important aspect to consider is the decomposition of Ni III G $_n$ complexes at pH higher than 9.0, so it was not possible the accurate data treatment.

The mechanism elucidation for the autoxidation of Co II G $_n$ complex is more complicated since species as mixed ligand complex and dimeric complexes with μ -superoxo bridges may be involved.

The redox cycling represented in the Scheme 1, involving changes in the oxidation state of the metal ion complex, is active as long as sulfite and oxygen are present in the solution to generate the SO $_5^{2-}$, HSO $_5^-$ and SO $_4^{2-}$ species.

The understanding of the redox cycling process of Ni III G $_n$ /Ni II G $_n$ and Co III G $_n$ /Co II G $_n$ is of interest not only in atmospheric processes but also in the treatment of gaseous effluents to assist pollution control systems development since these metal ion complexes can be efficient catalysts of sulfur compounds. Is necessary to mention also that DNA and RNA damage can be correlated with nickel and cobalt ion catalyzed S(IV) autoxidation.⁴⁸⁻⁵¹

Acknowledgments

The authors gratefully acknowledge the financial support from Fundação de Amparo à Pesquisa do Estado de São Paulo (FAPESP) and Conselho Nacional de Pesquisa e Desenvolvimento Tecnológico (CNPq) (Brazilian agencies).

References

1. Neves, E. A.; Coichev, N.; Gebert, J.; Klockow, D.; *Fresenius Z. Anal. Chem.* **1989**, 335, 386.
2. Coichev, N.; van Eldik, R.; *Inorg. Chem.* **1991**, 30, 2375.
3. Coichev, N.; van Eldik, R.; *Inorg. Chim. Acta* **1991**, 185, 69.
4. Leite, H. M. S.; Coichev, N.; Neves, E. A.; *Anal. Lett.* **1996**, 29, 2587.
5. Yoshida, D.; Moya, H. D.; Bonifácio, R. L.; Coichev, N.; *Spectrosc. Lett.* **1998**, 31, 1495.
6. Moya, H. D.; Neves, E. A.; Coichev, N.; *J. Chem. Educ.* **1999**, 76, 930.
7. Pezza, H. R.; Bonifácio, R. L.; Coichev, N.; *J. Chem. Res-M.* **1999**, 1520.
8. Pezza, H. R.; Coichev, N.; *J. Coord. Chem.* **1999**, 47, 107.
9. Lima, S.; Bonifácio, R. L.; Azzellini, G. C.; Coichev, N.; *Talanta* **2002**, 56, 547.
10. Alipázaga, M. V.; Bonifácio, R. L.; Kosminsky, L.; Bertotti, M.; Coichev, N.; *J. Braz. Chem. Soc.* **2003**, 14, 713.
11. Alipázaga, M. V.; Coichev, N.; *Anal. Lett.* **2003**, 36, 2255.
12. Lowinsohn, D.; Alipázaga, M. V.; Coichev, N.; Bertotti, M.; *Electrochim. Acta* **2004**, 49, 1761.
13. Lowinsohn, D.; Alipázaga, M. V.; Coichev, N.; Bertotti, M.; *Microchim. Acta* **2004**, 144, 57.
14. Bonifácio, R. L.; Coichev, N.; *Anal. Chim. Acta* **2004**, 517, 125.
15. Carvalho, L. B.; Alipázaga, M. V.; Crivelente, W. C. T.; Coichev, N.; *Inorg. React. Mech.* **2004**, 5, 101.
16. Alipázaga, M. V.; Moreno, R. G. M.; Coichev, N.; *Dalton Trans.* **2004**, 2036.
17. Alipázaga, M. V.; Lowinsohn, D.; Bertotti, M.; Coichev, N.; *Dalton Trans.* **2004**, 267.
18. Reddy, K. B.; Coichev, N.; van Eldik, R.; *J. Chem. Soc., Chem. Commun.* **1991**, 481.
19. Reddy, K. B.; van Eldik, R.; *Atmos. Environ.* **1992**, 26A, 661.
20. Bossu, F. P.; Paniago, E. B.; Margerum, D. W.; Kirksey, S. T.; Kurtz, J. L.; *Inorg. Chem.* **1978**, 17, 1034.
21. Laitinen, H. A.; *Chemical Analysis*, Mc. Graw Hill: New York, 1960, p. 410.
22. Flaschka, H. A.; *EDTA Titrations*, Pergamon Press: London, 1959, p. 78.
23. Sasso, M. G.; Quina, F. H.; Bechara, E. J. H.; *Anal. Biochem.* **1986**, 156, 239.

24. Margerum, D. W.; Dukes, G. R.; *Metal Ions in Biological Systems*, Helmut Siegel (Marcel Dekker Inc.): New York, 1974, vol. 1, ch. 5, p.157.
25. *Olis Kinfite Routines*, On-line Instruments Systems, Inc., Jefferson, GA, 1989.
26. *Pro-K.2000 Rapid Kinetics Systems*, PC Pro-K Software, Applied Photophysics Ltd., 1996.
27. Atkins, P. W.; *Physical Chemistry*, 3rd ed., Oxford Press: Oxford, 1986.
28. Anast, J. M.; Margerum, D. W.; *Inorg. Chem.* **1981**, *20*, 2319.
29. Behra, P.; Sigg, L.; *Nature* **1990**, *344*, 419.
30. van Eldik, R.; Coichev, N.; Bal Reddy, K.; Gerhard, A.; *Berichte Der Bunsen-Gesellschaft-Physical Chemistry Chemical Physics* **1992**, *96*, 478.
31. Berglund, J.; Fronaeus, S.; Elding, L. I.; *Inorg. Chem.* **1993**, *32*, 4527.
32. Brandt, C.; Fábrián, I.; van Eldik, R.; *Inorg. Chem.* **1994**, *33*, 687.
33. Coichev, N.; van Eldik, R.; *J. Chem. Educ.* **1994**, *71*, 767.
34. Connick, R. E.; Zhang, Y. X.; *Inorg. Chem.* **1996**, *35*, 4613.
35. Fronaeus, S.; Berglund, J.; Elding, L.; *Inorg. Chem.* **1998**, *37*, 4939.
36. Lepentsiotis, V.; Domagala, J.; Grgic, I.; van Eldik, R.; Muller, J. G.; Burrows, C. J.; *Inorg. Chem.* **1999**, *38*, 3500.
37. Green, B. J.; Tesfai, T. M.; Xie, Y.; Margerum, D. W.; *Inorg. Chem.* **2004**, *43*, 1463.
38. Lange, N. A.; *Lange's Handbook of Chemistry*, 11th ed., McGraw-Hill: New York, 1973.
39. Cavalheiro, E. T. G.; Plepis, A. M. D.; Chierice, G. O.; Neves, E. A.; *Polyhedron* **1987**, *6*, 1717.
40. Vogt, A.; Kufelnicki, A.; Jezowska-Trzebiatowska, B.; *Polyhedron* **1990**, *9*, 2567.
41. Vogt, A.; Kufelnicki, A.; Lesniewska, B.; *Polyhedron* **1994**, *13*, 1027.
42. Coichev, N.; van Eldik, R.; *New J. Chem.* **1994**, *18*, 123.
43. Coichev, N.; Reddy, K. B.; van Eldik, R.; *Atmos. Environ.* **1992**, *26A*, 2295.
44. Brandt, C.; van Eldik, R.; *Chem. Rev.* **1995**, *95*, 119.
45. Sada, E.; Kumazawa, H.; Hikosaka, H.; *Ind. Eng. Chem. Res.* **1987**, *26*, 2016.
46. Narita, E.; Sato, T.; Shioya, T.; Ikari, M.; Okabe, T.; *Industrial & Engineering Chemistry Product Research And Development* **1984**, *23*, 262.
47. Chang, S. G.; Littlejohn, D.; Linn, S.; *Environ. Sci. Technol.* **1983**, *17*, 649.
48. Shi, X. L.; *J. Inorg. Biochem.* **1994**, *56*, 155.
49. Burrows, C. J.; Muller, J. G.; *Chem. Rev.* **1998**, *98*, 1109.
50. Moreno, R. G. M.; Alipázaga, M. V.; Medeiros, M. H. G.; Coichev, N.; *Dalton Trans.* **2005**, 1101.
51. Alipázaga, M. V.; Moreno, R. G. M.; Linares, E.; Medeiros, M. H. G.; Coichev, N.; *Dalton Trans.* **2005**, 3738.

Received: April 17, 2006

Published on the web: October 5, 2006

FAPESP helped in meeting the publication costs of this article.